Equilibrative Nucleoside Transporter 3 Deficiency Perturbs Lysosome Function and Macrophage Homeostasis

Chia-Lin Hsu,[1] Weiyu Lin,[1] Dhaya Seshasayee,[1] Yung-Hsiang Chen,[2] Xiao Ding,[2] Zhonghua Lin,[3] Eric Suto,[3] Zhiyu Huang,[3] Wyne P. Lee,[3] Hyunjoo Park,[3] Min Xu,[3] Mei Sun,[4] Linda Rangell,[4] Jeff L. Lutman,[5] Sheila Ulufatu,[5] Eric Stefanich,[5] Cecile Chalouni,[4] Meredith Sagolla,[4] Lauri Diehl,[4] Paul Fielder,[5] Brian Dean,[2] Mercedesz Balazs,[3] Flavius Martin[1]*

Lysosomal storage diseases (LSDs) are a group of heterogeneous disorders caused by defects in lysosomal enzymes or transporters, resulting in accumulation of undegraded macromolecules or metabolites. Macrophage numbers are expanded in several LSDs, leading to histiocytosis of unknown pathophysiology. Here, we found that mice lacking the equilibrative nucleoside transporter 3 (ENT3) developed a spontaneous and progressive macrophage-dominated histiocytosis. In the absence of ENT3, defective apoptotic cell clearance led to lysosomal nucleoside buildup, elevated intralysosomal pH, and altered macrophage function. The macrophage accumulation was partly due to increased macrophage colony-stimulating factor and receptor expression and signaling secondary to the lysosomal defects. These studies suggest a cellular and molecular basis for the development of histiocytosis in several human syndromes associated with ENT3 mutations and potentially other LSDs.

Hematopoietic cells lack de novo nucleoside generation and thus rely on membrane transporters to acquire nucleosides required for DNA and RNA synthesis, signal transduction, and adenosine 5′-triphosphate production. Transmembrane equilibrative and concentrative nucleoside transporters (ENTs and CNTs) carry nucleosides and cytotoxic nucleoside analogs across membranes (*1*, *2*). The major source of nucleoside recycling is the degradation of nucleic acids, which is largely accomplished by histiocytes, the tissue macrophages. Macrophages are highly phagocytic cells of the immune system, which take up and degrade cellular debris within lysosomes (*3*). Although nucleoside uptake from the periphery by nucleoside transporters is well characterized (*4*), little is known about how nucleosides are exported from lysosomes where nucleic acid degradation occurs. In addition to substrate breakdown, lysosomes also participate in cellular function and metabolism (*5*). Patients with genetic defects in lysosomal hydrolyzing enzymes or transporters accumulate pathway metabolites that manifest in a variety of lysosomal storage diseases (LSDs) (*6*–*8*).

Because macrophages phagocytose and degrade the majority of dying cells and their nucleic acids, we hypothesized that a specific transporter (or transporters) equilibrating nucleosides out of lysosomes should be enriched in macrophages to facilitate nucleoside recycling. A quantitative polymerase chain reaction survey of the ENTs in immune cells showed the highest expression of ENT3 in macrophages (fig. S1). To investigate the roles of ENT3 in nucleoside transport, we generated ENT3 knockout ($ENT3^{-/-}$) mice (*9*) (fig. S2).

$ENT3^{-/-}$ mice developed spontaneous lymphadenopathy and splenomegaly by 8 weeks of age (Fig. 1, A and B) and had a significantly shorter life span compared to littermates (Fig. 1C). To investigate if any immune cell population was altered early in life, we examined 3-week-old animals and observed that the number of splenic macrophages was significantly increased in $ENT3^{-/-}$ compared to littermates (Fig. 1D and fig. S3). In contrast, no differences in splenic T and B cell numbers were found. Thus, ENT3 deficiency affects macrophage development and/or proliferation. Macrophage infiltration was observed in multiple organs of $ENT3^{-/-}$ mice, including spleen, liver, pancreas, intestine; exacerbated as animals aged (Fig. 1E and fig. S3); and progressed to histiocytic sarcoma in mice examined when moribund (fig. S4). To explore the mechanisms contributing to macrophage accumulation in $ENT3^{-/-}$ mice, we examined macrophage apoptosis, proliferation, and cell surface activation markers. The frequency of macrophages that stained positive for TUNEL (terminal deoxynucleotidyl transferase–mediated deoxyuridine triphosphate nick end labeling) was similar between wild-type and $ENT3^{-/-}$ mice, with increased absolute numbers of $TUNEL^{+}$ $ENT3^{-/-}$ macrophages (Fig. 1F). Cycling 5-bromo-2′-deoxyuridine–positive ($BrdU^{+}$) splenic macrophages were significantly increased in both frequency and numbers, indicating active cycling as well as extramedullary myelopoiesis in $ENT3^{-/-}$ mice (Fig. 1G and fig. S5). However, $ENT3^{-/-}$ mice had normal basal concentrations of inflammatory serum cytokines and their splenic macrophages had normal surface activation markers (figs. S6 and S7), suggesting that myelopoiesis was not caused by an acute inflammatory response. Furthermore, macrophage expansion was recapitulated in normal irradiated recipients transplanted with $ENT3^{-/-}$ bone marrow cells, suggesting that hematopoietic cell defects contributed to the enhanced myelopoiesis (Fig. 1H and fig. S3D).

We hypothesized that ENT3 is the nucleoside transporter crucial for lysosomal nucleoside export and its absence may affect the late endosomal-lysosomal system. $ENT3^{-/-}$ splenic macrophages had increased numbers of lysosomal-associated membrane protein 1 $(lamp\text{-}1)^{+}$ vesicles (Fig. 2A and fig. S8). Furthermore, electron microscopy (Fig. 2A) showed that $ENT3^{-/-}$ macrophage lysosomes were enlarged in size and contained undigested materials (Fig. 2B), accompanied with elevated intralysosomal pH (Fig. 2C). Thus, ENT3 deficiency causes lysosomal abnormalities in macrophages. To dissociate in vivo macrophage developmental abnormalities caused by ENT3 deficiency from functional defects, we used bone marrow–derived macrophage (BMDM) cultures for phenotypic and functional analyses. $ENT3^{-/-}$ and wild-type BMDMs had comparable surface marker phenotypes and lipopolysaccharide-induced cytokine responses, suggesting that $ENT3^{-/-}$ BMDMs were developmentally normal with respect to these parameters (fig. S9). We then examined phagocytosis, phagosome-lysosome fusion, and degradation of engulfed materials in BMDMs. By tracking fluorescently labeled bacteria, we found no significant impairment of phagocytosis or phagosome-lysosome fusion (fig. S10) in $ENT3^{-/-}$ BMDMs. However, when the BMDMs were incubated with apoptotic thymocytes or challenged with live bacteria to mimic in vivo macrophage functions, $ENT3^{-/-}$ BMDMs showed both delayed degradation of apoptotic thymocytes (Fig. 2D and fig. S10D) and bacterial killing (Fig. 2E), implying defects in lysosomal functions. To examine the in vivo functional consequences of $ENT3^{-/-}$ macrophage lysosomal perturbations, we challenged mice with lethal doses of *Listeria monocytogenes*. $ENT3^{-/-}$ animals succumbed to *L. monocytogenes* infection significantly earlier compared to wild-type littermates (Fig. 2F). In addition, pathogen load was significantly increased in spleen, liver, and kidney of infected $ENT3^{-/-}$ mice (fig. S10E). Thus, $ENT3^{-/-}$ macrophages appear to have dysfunctional lysosomes incapable of normal cellular functions and overall defense.

The observations of $ENT3^{-/-}$ macrophage lysosomal abnormalities prompted us to hypothesize that perturbed nucleoside trafficking causes lysosomal defects in $ENT3^{-/-}$ macrophages, as seen in other LSDs (*10*, *11*). Adenosine, a representative nucleoside, accumulated in whole-cell extracts and purified lysosomes derived from ex vivo splenic $ENT3^{-/-}$ macrophages (Fig. 3, A and B), suggesting that lack of ENT3 impairs lysosomal nucleoside export. To examine the cause of this phenomenon in $ENT3^{-/-}$ macrophages, we performed kinetic studies in BMDMs. Adenosine

[1]Immunology, Genentech Inc., 1 DNA Way, South San Francisco, CA 94080, USA. [2]Drug Metabolism and Pharmacokinetics, Genentech Inc., 1 DNA Way, South San Francisco, CA 94080, USA. [3]Translational Immunology, Genentech Inc., 1 DNA Way, South San Francisco, CA 94080, USA. [4]Pathology, Genentech Inc., 1 DNA Way, South San Francisco, CA 94080, USA. [5]Pharmacokinetics and Pharmacodynamics, Genentech Inc., 1 DNA Way, South San Francisco, CA 94080, USA.

*To whom correspondence should be addressed. E-mail: martin.flavius@gene.com

concentrations were similar between ENT3$^{-/-}$ and littermate BMDMs before stimulation; however, upon challenge with exogenous apoptotic thymocytes, accumulation of adenosine was observed in ENT3$^{-/-}$ BMDM whole-cell extracts (Fig. 3C) and purified lysosomal fraction (fig. S11). Intracellular nucleoside homeostasis could be restored in ENT3$^{-/-}$ BMDMs retrovirally reconstituted with wild-type mouse and human ENT3 (Fig. 3, D and E), but not by the human ENT3 mutant 427S identified in H syndrome patients (*12*) (Fig. 3E). Excessive lysosomal nucleosides could compete for free protons within the lysosome and lead to their alkalization (*13*). Indeed, coincident with adenosine accumulation, ENT3$^{-/-}$ BMDMs as well as human ENT3-mutant 427S–expressing BMDMs challenged with apoptotic thymocytes had elevated intralysosomal pH (Fig. 3F and fig. S12). Thus, in the absence of ENT3, excess accumulation of nucleosides in lysosomes led to perturbed lysosomal functions and homeostasis of macrophages.

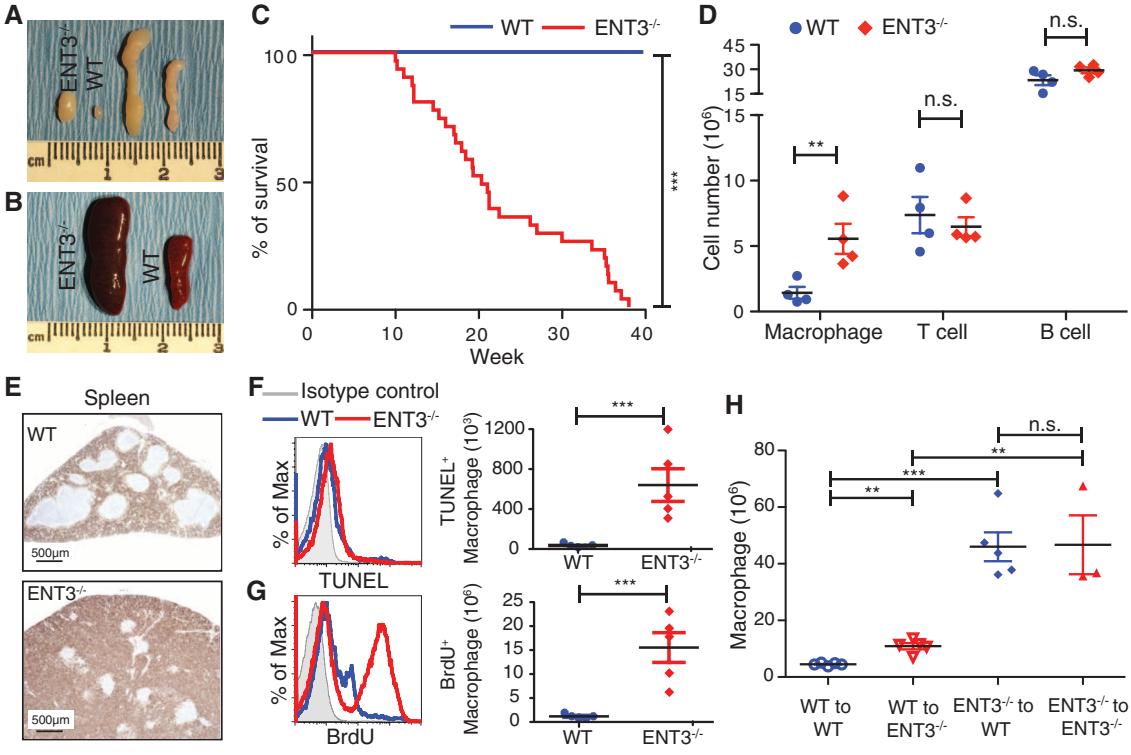

Fig. 1. ENT3 deficiency leads to histiocytosis. Photographs of 8-week-old inguinal and mesenteric lymph nodes (**A**) and spleen (**B**). (**C**) Life span of ENT3$^{-/-}$ and wild-type littermates (n = 30). (**D**) Splenic cellularity of 3-week-old mice (n = 4). (**E**) Spleen immunohistochemistry (F4/80 antibody staining). (**F**) Splenic macrophages undergoing apoptosis were analyzed by flow-cytometry (left) and quantified (right). (**G**) Proliferation of splenic macrophages was examined by flow cytometry (left) and quantified (right) (n = 5). (**H**) Splenic macrophages in radiation bone marrow chimeras of ENT3$^{-/-}$ and wild-type littermates (n = 3 to 5). $^{**}P < 0.05$, $^{***}P < 0.001$ (unpaired two-tailed t test); n.s., no significant difference. Error bars represent SEM.

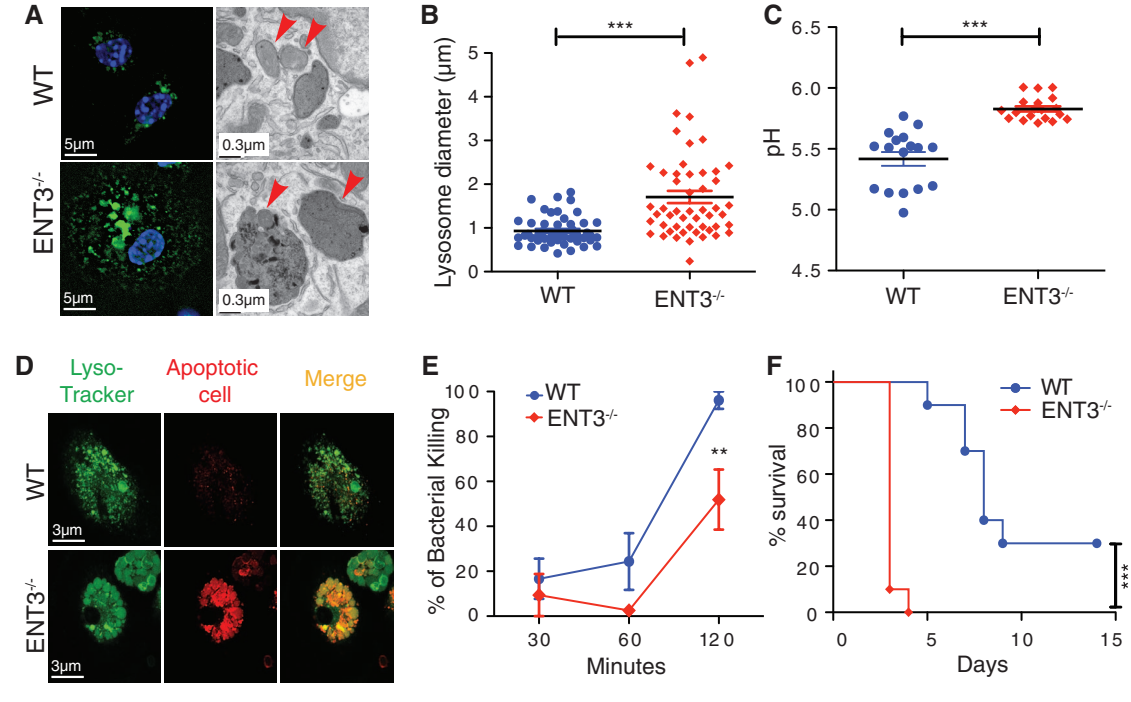

Fig. 2. ENT3 deficiency causes morphological and functional changes in macrophages. (**A**) (Left) Ex vivo splenic macrophages show increased lamp1 expression (green) and (right) electron microscopy showing undigested materials in ENT3$^{-/-}$ splenic macrophage lysosomes (red arrowheads). (**B**) Lysosome diameters. (**C**) Intralysosomal pH in splenic macrophages (n = 17 individual cells; representative of three independent experiments). (**D**) Processing of engulfed apoptotic thymocytes in BMDMs (24 hours). (**E**) In vitro bacterial killing assay of *Escherichia coli* with BMDMs. (**F**) *Listeria monocytogenes*–induced mortality (2×10^6 CFU, given intravenously) in wild-type littermates and ENT3$^{-/-}$ animals (n = 10). Statistics were done by unpaired t test or Mantel-Cox test. $^{**}P < 0.05$, $^{***}P < 0.001$; n.s., no significant difference. Error bars represent SEM.

Next, we investigated pathways that could drive ENT3$^{-/-}$ myeloproliferation and looked for perturbations in macrophage growth factor levels or their cognate receptors. Surface expression of macrophage colony-stimulating factor receptor (M-CSFR) was significantly higher in ENT3$^{-/-}$ splenic macrophages (Fig. 4A), whereas levels of the β-chain subunit of granulocyte-macrophage colony-stimulating factor (GM-CSFR) and fms-like tyrosine kinase receptor-3 (Flt3) were comparable to those of wild-type macrophages (fig. S13). In addition, ENT3$^{-/-}$ mice had elevated serum concentrations of M-CSF, although G-CSF, Flt3L, and IL-34 serum concentrations were normal (Fig. 4B and fig. S13). The high levels of M-CSF and its cognate receptor were accompanied by increased signaling through M-CSFR indicated by the phosphorylation status of Y723 of M-CSFR (*14*) in ENT3$^{-/-}$ macrophages (fig. S14). The higher M-CSF concentration was not due to increased production of M-CSF by ENT3$^{-/-}$ splenic and bone marrow stromal cells or macrophages (fig. S15), but more likely a result of defective M-CSF clearance (fig. S16). M-CSFR transcription was also similar between splenic ENT3$^{-/-}$ and wild-type macrophages (fig. S17), suggesting a posttranslational alteration of M-CSFR in ENT3$^{-/-}$ mice.

To assess the contribution of elevated M-CSF/M-CSFR axis to the accumulation of macrophages in ENT3$^{-/-}$ mice, we blocked this pathway using a neutralizing antibody against M-CSF (anti–M-CSF). After 4 or 24 weeks of treatment, ENT3$^{-/-}$ mice had 50% fewer splenic macrophages compared to the isotype control antibody-treated group (Fig. 4C and figs. S18 and S19). Anti–M-CSF treatment in ENT3$^{-/-}$ mice also resulted in lower granulocyte and macrophage CFU numbers but not Ki67^{+} cycling splenic macrophages (figs. S18 and S19), suggesting that the M-CSF/M-CSFR axis participates in myeloproliferation primarily through enhanced extramedullary myelopoiesis. In addition, ENT3$^{-/-}$ splenic macrophages had elevated and sustained M-CSFR expression even after anti–M-CSF treatment (fig. S18), supporting the hypothesis that ENT3$^{-/-}$ macrophages have a posttranslational modification of M-CSFR that is independent of ligand engagement. M-CSF blockade did not alter the mortality seen in ENT3$^{-/-}$ mice (fig. S19), suggesting that the residual histiocytosis and mortality involve factors beyond surveyed myeloid growth factors (fig. S13).

To understand why M-CSF blockade rescued only partially the ENT3$^{-/-}$ histiocytosis phenotype, we investigated factors that may be affected by impaired macrophage functions and found accumulation of apoptotic cells in the spleen after anti–M-CSF treatment (fig. S19). Because exogenous apoptotic cell burden induces lysosomal dysfunctions in the ENT3$^{-/-}$ macrophages (Fig. 3, C and F), we asked if its removal could prevent histiocytosis. In mixed bone marrow chimeras, the presence of wild-type bone marrow cells alleviated the macrophage expansion phenotype and removed apoptotic cells in a dose-dependent manner (Fig. 4D and fig. S20). Furthermore, the M-CSFR surface expression on ENT3$^{-/-}$ macrophages reverted to normal in the presence of ENT3-competent cells (Fig. 4E). To examine whether the exogenous nucleic acid pressure directly affects M-CSFR turnover, we stressed BMDMs with apoptotic thymocytes and found that surface expression of M-CSFR was increased in ENT3$^{-/-}$ compared with wild-type BMDMs (Fig. 4F and fig. S21). Moreover, ligand-induced M-CSFR endocytosis appear similar between wild-type and ENT3$^{-/-}$ BMDMs (fig. S22). Thus, the dysregulation of M-CSFR turnover in ENT3$^{-/-}$ cells is ligand-independent and a consequence of exogenous nucleic acid pressure. Because the down-regulation of M-CSFR and termination of M-CSF/M-CSFR signaling rely ultimately on lysosomal degradation (*15*, *16*), we examined whether lysosomal alkalization can explain the M-CSFR dysregulation in ENT3$^{-/-}$ animals. By treating wild-type BMDM with bafilomycin, a lysosomal pH-altering agent, we found that lysosomal alkalization leads to higher surface expression and less degradation of M-CSFR (Fig. 4, G and H). These data provide a causative link between lysosomal nucleoside accumulation and alkalization to dysregulated M-CSFR turnover and signaling.

Here, we have identified ENT3 as an essential transmembrane transporter to maintain lysosome integrity by regulating nucleoside trafficking. ENT3 deficiency, through defects in the lysosomal system, caused ineffective apoptotic cell clearance and increased M-CSF signaling that contribute to elevated numbers of macrophages and histiocytosis. Loss-of-function human ENT3 mutants have recently been associated with familial Rosai-Dorfman disease, Faisalabad histiocytosis, H syndrome, and pigmented hypertrichosis with insulin-dependent diabetes (*12*, *17*–*21*), diseases that in some cases have lymphadenopathy, splenomegaly, and increased infiltration of macrophages in various immune and nonimmune organs. Our findings provide the cellular and molecular mechanism for the histiocytosis seen in these patients and potentially other LSDs. We can envisage that this mechanism, resulting in impaired dead cell removal and M-CSF/M-CSFR dysfunction

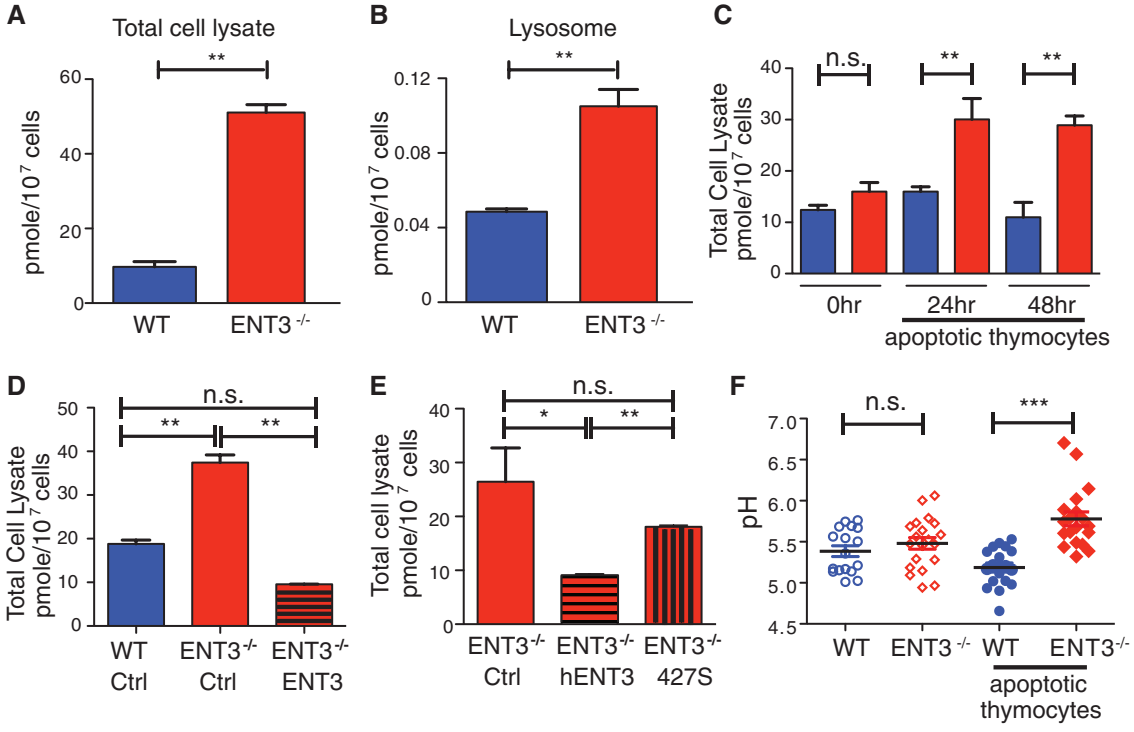

Fig. 3. Lysosomal nucleoside accumulation and pH increase in ENT3$^{-/-}$ macrophages. Intracellular adenosine concentrations from splenic macrophage whole-cell lysate (**A**) or enriched lysosomes (**B**) ($n = 3$). (**C**) Intracellular adenosine concentrations in BMDMs challenged with apoptotic thymocytes. (**D** and **E**) Intracellular adenosine in retrovirally transduced BMDMs after incubation with apoptotic thymocytes. (**F**) Intralysosomal pH values of BMDMs at 48 hours after incubation with apoptotic thymocytes. Data in (A to C) and (D to F) are representative of three and two independent experiments, respectively. $^{**}P < 0.05$, $^{***}P < 0.001$; n.s., no significant difference. Error bars represent SEM.

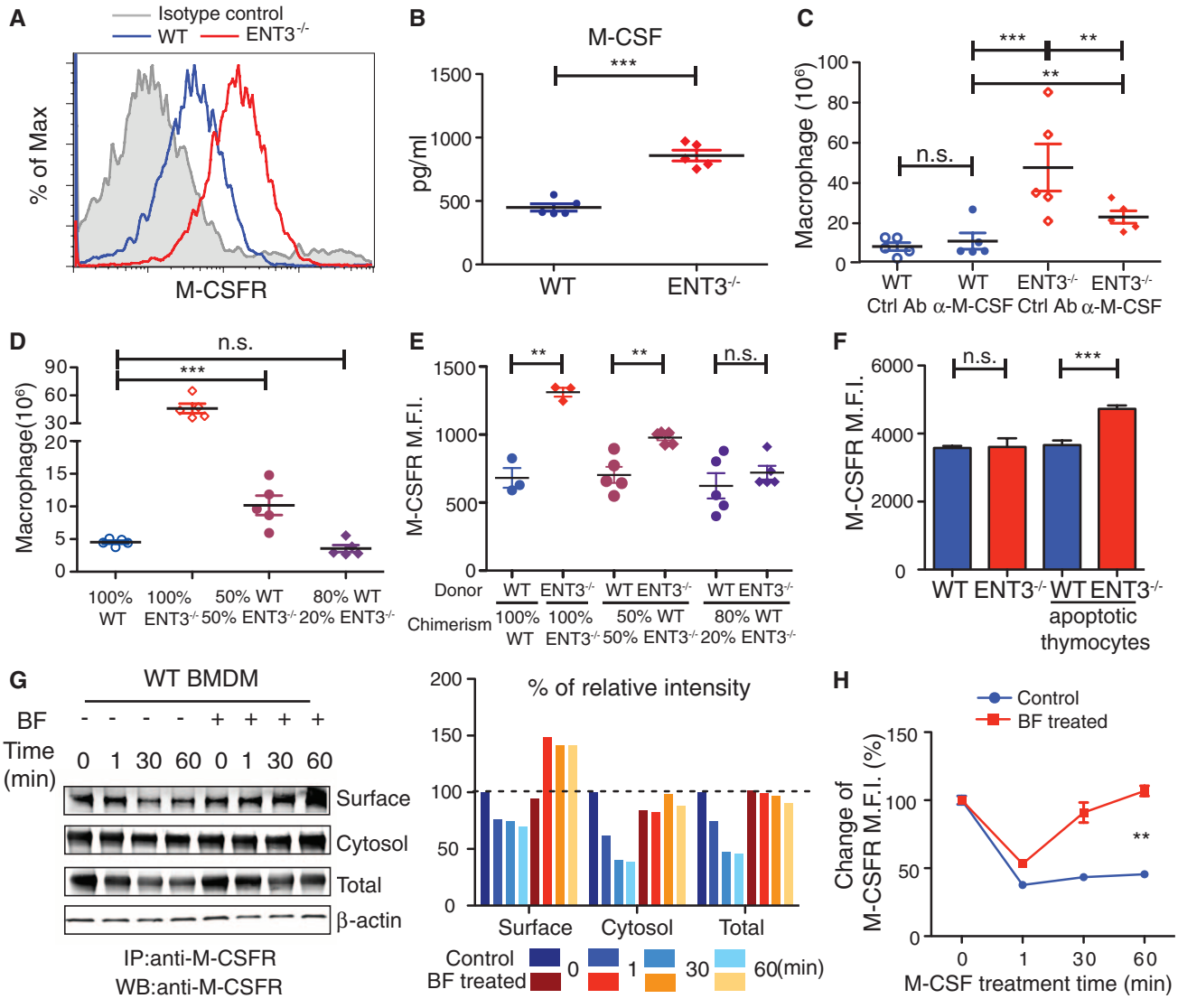

Fig. 4. Altered M-CSF/M-CSF receptor axis contributes to the myeloproliferative phenotype in ENT3$^{-/-}$ animals. (**A**) Surface expression of M-CSFR on splenic macrophages. (**B**) Serum concentrations of M-CSF (12 weeks, $n = 5$). (**C**) Splenic macrophage numbers after 4 weeks of treatment with neutralizing anti–M-CSF or control antibodies ($n = 5$). Number of splenic macrophages (**D**) and quantification of surface M-CSFR (**E**) in wild-type-ENT3$^{-/-}$ mixed bone marrow chimera mice ($n = 3$ to 5 per group). Decrease in average M-CSFR surface expression occurs in ENT3$^{-/-}$ macrophages. (**F**) M-CSFR surface expression on BMDMs upon apoptotic thymocyte challenge (72 hours, $n = 3$). (**G**) Immunoblot analysis (left) and quantification (right) of M-CSFR turnover on wild-type BMDMs after bafilomycin treatment. (**H**) Flow cytometric analysis of surface M-CSFR turnover with bafilomycin treatment ($n = 3$). *P* values were determined by unpaired *t* test. $^{**}P < 0.05$, $^{***}P < 0.001$; n.s., no significant difference. Error bars represent SEM.

and histiocytosis, may be contributing pathways for a broader range of lysosomal storage diseases, independent of ENT3 mutations.

References and Notes

1. S. A. Baldwin *et al.*, *Pflugers Arch.* **447**, 735 (2004).
2. M. Molina-Arcas, F. J. Casado, M. Pastor-Anglada, *Curr. Vasc. Pharmacol.* **7**, 426 (2009).
3. D. G. Russell, B. C. Vanderven, S. Glennie, H. Mwandumba, R. S. Heyderman, *Nat. Rev. Immunol.* **9**, 594 (2009).
4. J. D. Young, S. Y. Yao, L. Sun, C. E. Cass, S. A. Baldwin, *Xenobiotica* **38**, 995 (2008).
5. P. Saftig, J. Klumperman, *Nat. Rev. Mol. Cell Biol.* **10**, 623 (2009).
6. E. B. Vitner, F. M. Platt, A. H. Futerman, *J. Biol. Chem.* **285**, 20423 (2010).
7. G. M. Mancini, A. C. Havelaar, F. W. Verheijen, *J. Inherit. Metab. Dis.* **23**, 278 (2000).
8. A. H. Futerman, G. van Meer, *Nat. Rev. Mol. Cell Biol.* **5**, 554 (2004).
9. T. Tang *et al.*, *Nat. Biotechnol.* **28**, 749 (2010).
10. A. Fraldi *et al.*, *EMBO J.* **29**, 3607 (2010).
11. T. Fukuda *et al.*, *Ann. Neurol.* **59**, 700 (2006).
12. N. Kang *et al.*, *J. Biol. Chem.* **285**, 28343 (2010).
13. B. Poole, S. Ohkuma, *J. Cell Biol.* **90**, 665 (1981).
14. T. G. Douglass *et al.*, *Int. Immunopharmacol.* **8**, 1354 (2008).
15. A. Bartocci *et al.*, *Proc. Natl. Acad. Sci. U.S.A.* **84**, 6179 (1987).
16. P. S. Lee *et al.*, *EMBO J.* **18**, 3616 (1999).
17. E. Avitan-Hersh *et al.*, *Am. J. Dermatopathol.* **33**, 47 (2011).
18. V. Molho-Pessach *et al.*, *Am. J. Hum. Genet.* **83**, 529 (2008).
19. N. V. Morgan *et al.*, *PLoS Genet.* **6**, e1000833 (2010).
20. S. T. Cliffe *et al.*, *Hum. Mol. Genet.* **18**, 2257 (2009).
21. R. Spiegel *et al.*, *Eur. J. Med. Genet.* **53**, 309 (2010).

Acknowledgments: We thank N. Nakamura, I. Mellman, A. Chan, W. Ouyang, M. van Lookeren-Campagne, E. Brown, and H. Singh for discussions and critical reading of the manuscript; J. Cupp, A. Martinez, and the flow cytometry group for cell sorting and Luminex analysis; J. Zhang, M. Zhou, and P. Gribling, for animal studies; J. Ding for cloning support; and D. Delarosa and J. Young for M-CSF detection assay. Authors are employees of Genentech, a member of the Roche group. The data are presented in the figures and in the SOM.

Supporting Online Material

www.sciencemag.org/cgi/content/full/science.1213682/DC1
Materials and Methods
Figs. S1 to S24
References

7 September 2011; accepted 21 November 2011
Published online 15 December 2011;
10.1126/science.1213682

Science

Equilibrative Nucleoside Transporter 3 Deficiency Perturbs Lysosome Function and Macrophage Homeostasis

Chia-Lin Hsu, Weiyu Lin, Dhaya Seshasayee, Yung-Hsiang Chen, Xiao Ding, Zhonghua Lin, Eric Suto, Zhiyu Huang, Wyne P. Lee, Hyunjoo Park, Min Xu, Mei Sun, Linda Rangell, Jeff L. Lutman, Sheila Ulufatu, Eric Stefanich, Cecile Chalouni, Meredith Sagolla, Lauri Diehl, Paul Fielder, Brian Dean, Mercedesz Balazs and Flavius Martin

Science **335** (6064), 89-92.
DOI: 10.1126/science.1213682originally published online December 15, 2011

From Nucleoside Recycling to Histiocytosis

Macrophages remove billions of apoptotic cells daily, releasing their nucleic acid material through lysosomal degradation, which allows the resulting nucleosides to be recycled. **Hsu *et al.*** (p. 89, published online 15 December) found that the nucleoside transporter, equilibrative nucleoside transporter 3 (ENT3), was highly expressed in macrophages and showed that mice deficient in this transporter develop histiocytosis and features of lysosomal storage disease. When exposed to apoptotic cells, macrophages carrying human ENT3 mutations accumulated adenosine and increased their lysosomal pH. These changes contributed to an enhanced signaling through macrophage colony-stimulating factor (M-CSF) receptor and, ultimately, to M-CSF–driven myeloproliferative disease.

Science (print ISSN 0036-8075; online ISSN 1095-9203) is published by the American Association for the Advancement of Science, 1200 New York Avenue NW, Washington, DC 20005.